Paper published on:
Solar Energy Materials and Solar Cells, Vol. 161 (2017), pages 1-6,
http://dx.doi.org/10.1016/j.solmat.2016.10.054
http://www.sciencedirect.com/science/article/pii/S092702481630469X

Effect of surface texturing by femtosecond laser on tantalum carbide ceramics for solar receiver applications

D. Sciti, D.M. Trucchi, A. Bellucci, S. Orlando, L. Zoli, E. Sani *

CNR-ISTEC, Institute of Science and Technology for Ceramics, Via Granarolo 64, I-48018 Faenza (Italy)
CNR-ISM, Institute of Structure of Matter - Montelibretti Section, Via Salaria km 29.300, I-00015 Monterotondo Scalo (Italy)
CNR-INO, National Institute of Optics, Largo E. Fermi, 6, I-50125 Firenze, Italy
*Corresponding author: elisa.sani@ino.it

Abstract
Tantalum carbide, as a Ultra-High Temperature Ceramic, is known to be characterized by intrinsic spectral selectivity, which makes it attractive for novel high-temperature thermal solar absorbers. However, a weakness point of TaC is the solar absorbance, which, in absence of any treatment, is usually lower than that of other materials currently under development for solar absorber applications. In the present work we have investigated the effect of surface texturing by femtosecond laser machining on this superhard material. Laser-induced microstructural and optical property changes have been characterized in two samples with different starting roughness and for four laser treatments each, as a function of the accumulated laser fluence. As the interaction with the laser beam takes place and gets stronger, both surface and chemical composition changes appear. Optical properties are heavily affected: solar absorbance considerably increases, at a slight expense of spectral selectivity.

Keywords: Tantalum carbide, ceramic, solar absorber, femtosecond laser, surface patterning

1. Introduction

Sunlight is a free and abundant energy source and technologies exploiting it are experiencing an impressive development. Among them, concentrating solar power (CSP) is considered one of the most promising. In the classical scheme of CSP, electrical power is produced by a thermodynamic conversion driven by the heat transfer to a fluid (water, steam, molten salts) activating thermal engines [1]. Recent advances propose hybrid concepts like combined thermal-thermionic technologies [2]. In all cases, a high solar absorbance is the main parameter required to the sunlight receiver material, while thermal emission losses are minimized by a good spectral selectivity [3]. On the other hand, it should be noticed that basics of physics states that the efficiency of thermal cycles increases with temperature. Thus, the present main challenge for thermodynamic solar energy exploitation is to find a receiver material able to allow higher operating temperatures than current systems (usually limited to 800 K or lower) [4,5], while showing the favorable optical properties mentioned above as well as good thermal and mechanical characteristics.

Recent studies on ultra-high temperature ceramics (UHTCs) have shown that carbides and borides of tantalum, hafnium and zirconium possess, besides other favorable characteristics like high thermal conductivity high hardness and strength and the highest melting points of any known material, also good spectral selectivity and low emittance at high temperatures [6-15]. The main weakness of these carbides is their poor resistance to oxidation, so they are primarily proposed for operation in vacuum,

Paper published on:
Solar Energy Materials and Solar Cells, Vol. 161 (2017), pages 1-6,
http://dx.doi.org/10.1016/j.solmat.2016.10.054
http://www.sciencedirect.com/science/article/pii/S092702481630469X

like in the device described in [16], or under inert atmosphere. However, it should be emphasized that the introduction of secondary phases able to produce silica-based glass (like SiC, $MoSi_2$, $TaSi_2$ and all transition-metal silicides) greatly improves their oxidation resistance [17,18]. Tantalum carbide (TaC) has been recently studied by our group [7,8,19] and its intrinsic thermal selectivity and low thermal emittance have been proven. As a term of comparison, it should be considered that the ideal solar absorber should have a low emittance at thermal infrared wavelengths and a high absorbance at wavelengths of solar spectrum. Generally speaking, UHTCs already fairly satisfy the first requirement, even with some differences among them, while the second requirement is more critical. For instance, for TaC, the integrated solar absorbance has been estimated to be around 0.4 for optically smooth surfaces and around 0.5 for porous specimens [8,19]. A typical approach to increase the absorbance is to create a surface periodic pattern, able to capture the optical radiation [5,20] (i.e. decreasing the reflectance). However, patterning through conventional ceramic processing techniques is a difficult task for superhard UHTC materials. Laser machining is a flexible and non-contact technique particularly suited for producing surface textures [21-29]. The possibility to control the surface processing parameters (wavelength, fluence, number and duration of pulses, spot size, beam homogeneity, beam angle of incidence, ambient pressure) allows the achievement of tailored surface structures. Short and ultra-short pulse lasers have been investigated in the literature for machining structures in a variety of solid materials [30,31,32]. However, the obtained surface modifications on ceramic samples strictly depend on material-related factors, such as microstructure, composition, optical absorption coefficient and thermal conductivity [21-29], besides on parameters of the laser radiation itself. Very recently, femtosecond laser patterning has been demonstrated to increase the solar absorbance of hafnium carbide [33]. In this work a femtosecond laser is used to produce a regular pattern on TaC materials. We report on the optimization of the laser machining of this superhard and ultra-high temperature ceramic, to obtain a regular surface texture particularly useful for increasing the solar absorbance. The morphological aspects characterizing the material are analysed, as well as optical properties in the spectral range 0.3-15.5 μm.

2. Materials and methods

The monolithic TaC was produced by hot pressing at 1900 °C and contains a residual porosity of approximately 5 vol%. Details on the material processing are reported in [17]. From the sintered pellets, two discs of approximately 4 cm diameter were prepared by conventional diamond machining on both sides: the first disc was finished down to 0.2 μm and the second disc down to 1.0 μm surface roughness (labelled as T0.2 and T1 in Table I, respectively). One of the sides of each sample was left as reference for the untreated material. The other side was divided into four approximately equal areas, and each of them undergone a different femtosecond laser treatment.

The laser system employed for the surface texturing is based on a Spectra Physics Tsunami S - fs oscillator (pulse duration of about 100 fs, repetition rate 80 MHz, wavelength 800 nm, peak power > 0.7 W) pumped by a Spectra-Physics Millennia Pro 5sJS (continuous wave (CW) diode, wavelength 532 nm, power 5W). The output of the oscillator is the seed for the Spectra-Physics Spitfire Pro 100 F 1K XP 4W amplifier (pulse duration < 120 fs, repetition rate selectable in the range 1 – 1000 Hz, wavelength 800 nm, pulse energy up to 4 mJ/pulse) pumped by a Spectra-Physics Empower 30 Q-switched Diode Pumped Solid State Nd:YLF. Figure 1 shows the schematic of the experimental setup.

Paper published on:
Solar Energy Materials and Solar Cells, Vol. 161 (2017), pages 1-6,
http://dx.doi.org/10.1016/j.solmat.2016.10.054
http://www.sciencedirect.com/science/article/pii/S092702481630469X

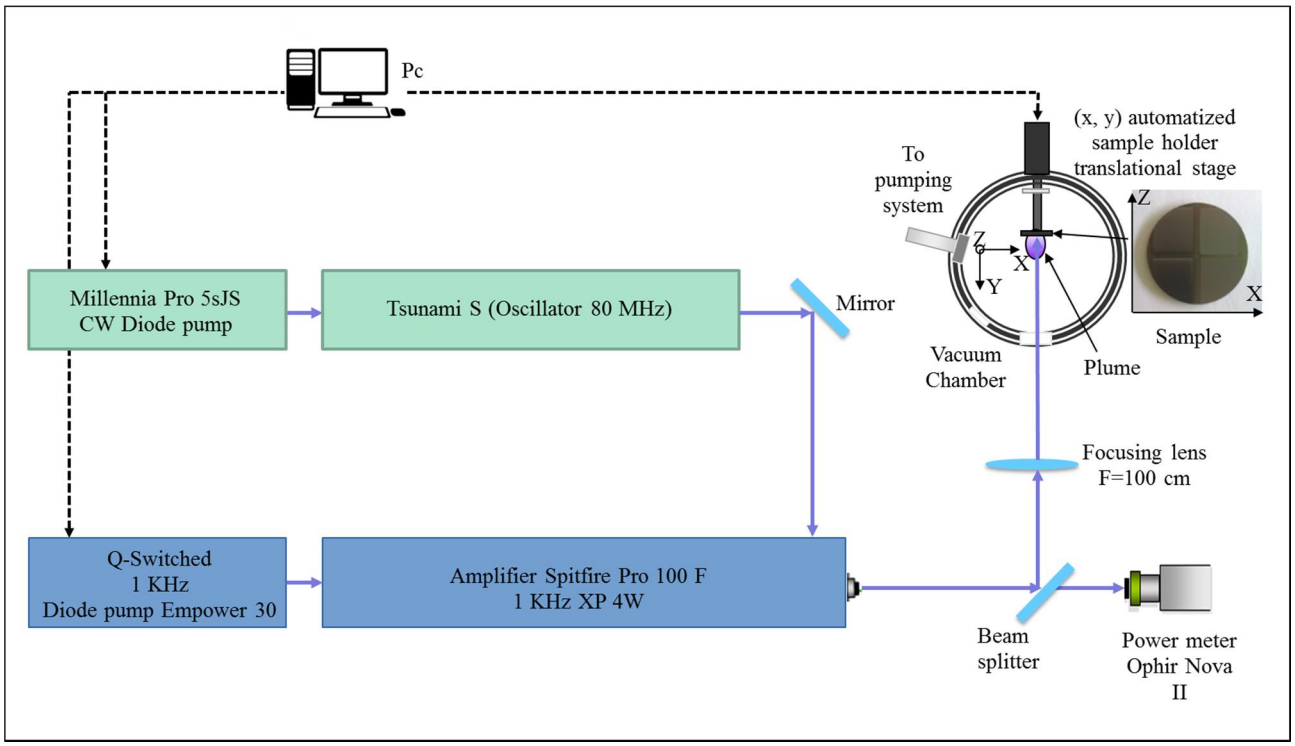

Figure 1: Schematic of the laser processing system. The CW diode acts as a pump for the oscillator, whose output is the seed for the light amplifier, pumped by the Q-switched diode. The beam is then splitted to allow a power-meter to control the pulse energy, whereas a lens with focal length of 100 cm focuses the beam on the sample-holder plane (X, Z), situated within a vacuum chamber. The sample, that produces a small plume under laser beam illumination, is moved along X and Z axes during the surface treatment.

The horizontally polarized laser beam was focused perpendicularly to the sample surface with a wavelength of 800 nm and a pulse energy of 3.6 mJ/pulse, kept constant for all the experiments and measured with a power-meter Ophir Nova II coupled to a thermal head Ophir 30(150)A-LP1. The TaC target was installed in a high vacuum chamber (pressure $<4\times10^{-7}$ mbar) and moved according to a raster path by an automated X-Z translational stage along the two directions orthogonal to the laser axis with selectable speed. The translational speed produces a pulse-to-pulse distance (pitch) and an overlap over the X and Z axes [34]. A variation of the translational speed induces a variation of the total accumulated fluence per surface unit that we define as the number of pulses multiplied to the constant pulse energy. The gaussian laser beam was found to produce a modification region on the sample of 250 µm diameter and an ablation one of about 150 µm [35,36].

The different zones of the TaC samples were processed with a different longitudinal translational speed, ranging from 0.56 to 5.63 mm/s (Table I), whereas the vertical speed was kept constant to the value of about 2.0 mm/s for a translation of 0.15 mm, approximately equal to the ablation diameter. With a laser repetition rate kept constant at 1 kHz, the speed variation corresponded to a longitudinal pitch ranging from 0.6 to 5.6 µm and an associated strong longitudinal overlap from about 99.6% down to 96.2%. The total accumulated fluence per unit area ranged from 0.43 to 4.28 kJ/cm^2, namely each point of the sample surface was impinged by an average number of pulses ranging approximately from 21 to 210. The treated surfaces are listed in Table I.

Paper published on:
Solar Energy Materials and Solar Cells, Vol. 161 (2017), pages 1-6,
http://dx.doi.org/10.1016/j.solmat.2016.10.054
http://www.sciencedirect.com/science/article/pii/S092702481630469X

After laser treatments, for treated and as polished surfaces, the mean surface roughness (R_a) and the distance between the highest asperity, peak or summit, and the lowest valley (R_t) was measured according to the European standard CEN 624-4 using a commercial contact stylus instrument (Taylor Hobson mod. Talysurf Plus) fitted with a 2 µm-radius conical diamond tip over a track length of 8 mm and with a cut-off length of 0.8 mm. A standard procedure for surface finishing was adopted to exclude any influence of polishing time, pressure and grade. The microstructural features of as polished and treated samples were detected by scanning electron microscopy (FE-SEM, Carl Zeiss Sigma NTS Gmbh, Oberkochen, DE) and energy dispersive X-ray spectroscopy (EDS, INCA Energy 300, Oxford instruments, UK).

Sample label	x- speed (mm/s)	Accumulated fluence per unit area (kJ/cm^2)	R_a (µm)	R_t (µm)
T0.2tq	----	----	0.20±0.02	1.18±0.14
T0.2#4	5.63	0.43	0.32±0.04	1.83±0.27
T0.2#3	2.81	0.85	0.31±0.04	1.78±0.27
T0.2#2	1.13	2.12	0.51±0.04	2.68±0.28
T0.2#1	0.56	4.28	0.99±0.10	4.52±0.61
T1tq	----	----	1.06±0.09	5.43±0.52
T1#4	5.63	0.43	1.19±0.15	6.22±0.77
T1#3	2.81	0.85	1.57±0.12	8.61±0.81
T1#2	1.13	2.12	2.07±0.34	10.48±1.88
T1#1	0.56	4.28	1.92±0.14	9.60±0.84

Table I: Investigated samples. T-0.2 and T-1 indicate surfaces with original finishing to 0.2 and 1.0 µm, respectively. For both discs, letters tq label untreated surfaces. The final number appearing in labels is connected to the laser treatment, from 4 (surfaces with the shortest time interaction with laser: lightest treatment) to 1 (surfaces with the longest interaction).

Optical reflectance spectra at room temperature in the 0.25 - 2.5 µm wavelength region were acquired using a double-beam spectrophotometer (Perkin Elmer "Lambda900") equipped with a 150-mm diameter integration sphere for the measurement of the hemispherical reflectance. The spectra in the wavelength region 2.5 - 15.5 µm have been acquired using a Fourier Transform spectrophotometer (FT-IR Bio-Rad "Excalibur") equipped with a gold-coated integrating sphere and a liquid nitrogen-cooled detector. In all cases the reflectance spectra are acquired for quasi-normal incidence angle.

Paper published on:
Solar Energy Materials and Solar Cells, Vol. 161 (2017), pages 1-6,
http://dx.doi.org/10.1016/j.solmat.2016.10.054
http://www.sciencedirect.com/science/article/pii/S092702481630469X

3. Results

Microstructure and roughness

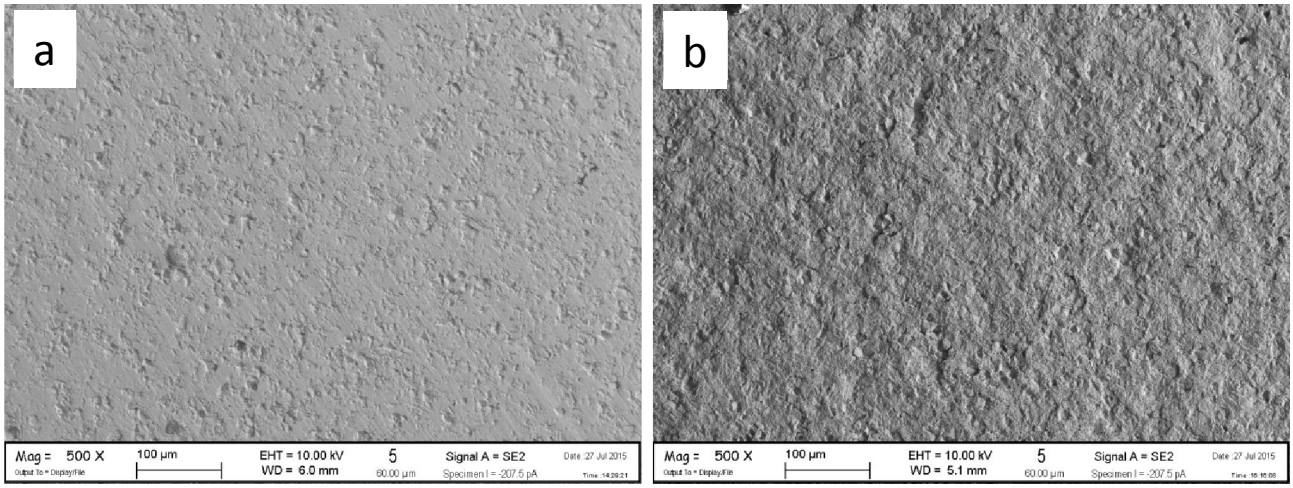

Figure 2: As polished surfaces for TaC monolithic materials. a) T0.2tq, b) T1tq

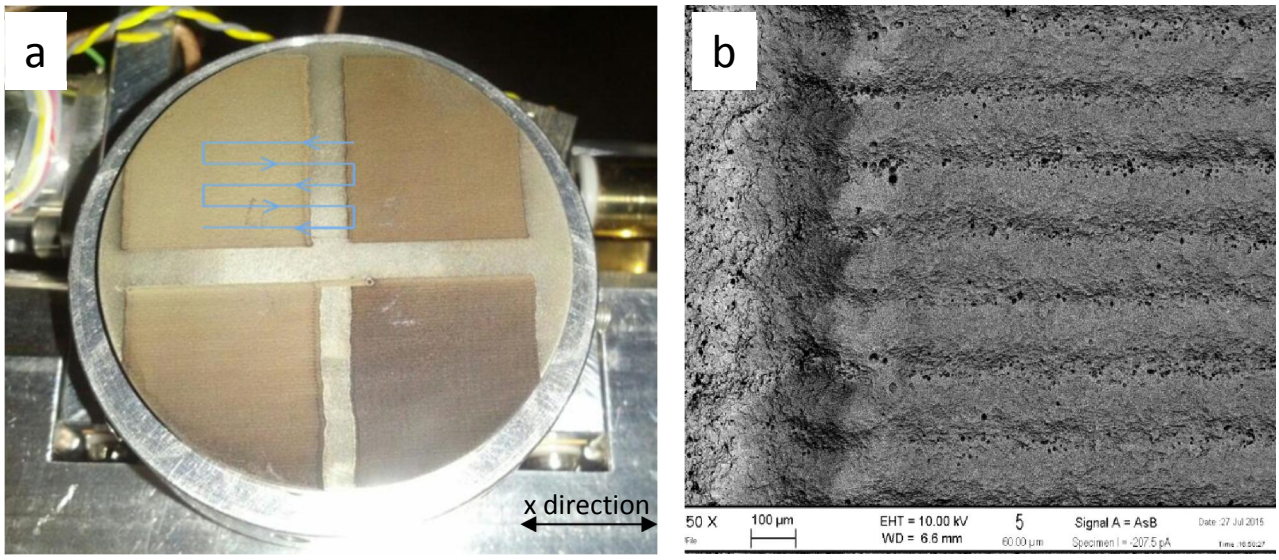

Figure 3: a) picture of the TaC pellet (treated side). Blue lines indicate the bustrophedic path of the laser (x-direction: parallel to grooves, z-direction: perpendicular to grooves). Treated sections are separated each other by untreated strips. b) SEM image of the grooves created by the laser scan

Figure 2 illustrates the typical bulk morphology of these samples before the laser treatment, showing the different starting surface roughness of the two samples. Isolated pores are found in the microstructure with dimensions in the range 0.3–1 µm, typical mean grain size of these ceramics is 10-20 µm [7]. Visual inspection (see Figure 3a) after the laser treatment reveals a change of colour in the treated areas, with a clear tendency of the surface to darken with decrease of the laser speed. The laser path creates a series of macro-grooves which are visible in Figure 3b. Inside each groove,

Paper published on:
Solar Energy Materials and Solar Cells, Vol. 161 (2017), pages 1-6,
http://dx.doi.org/10.1016/j.solmat.2016.10.054
http://www.sciencedirect.com/science/article/pii/S092702481630469X

a submicrometric pattern constituted by periodic ripples is created, with elongated features disposed perpendicular to the laser scan direction

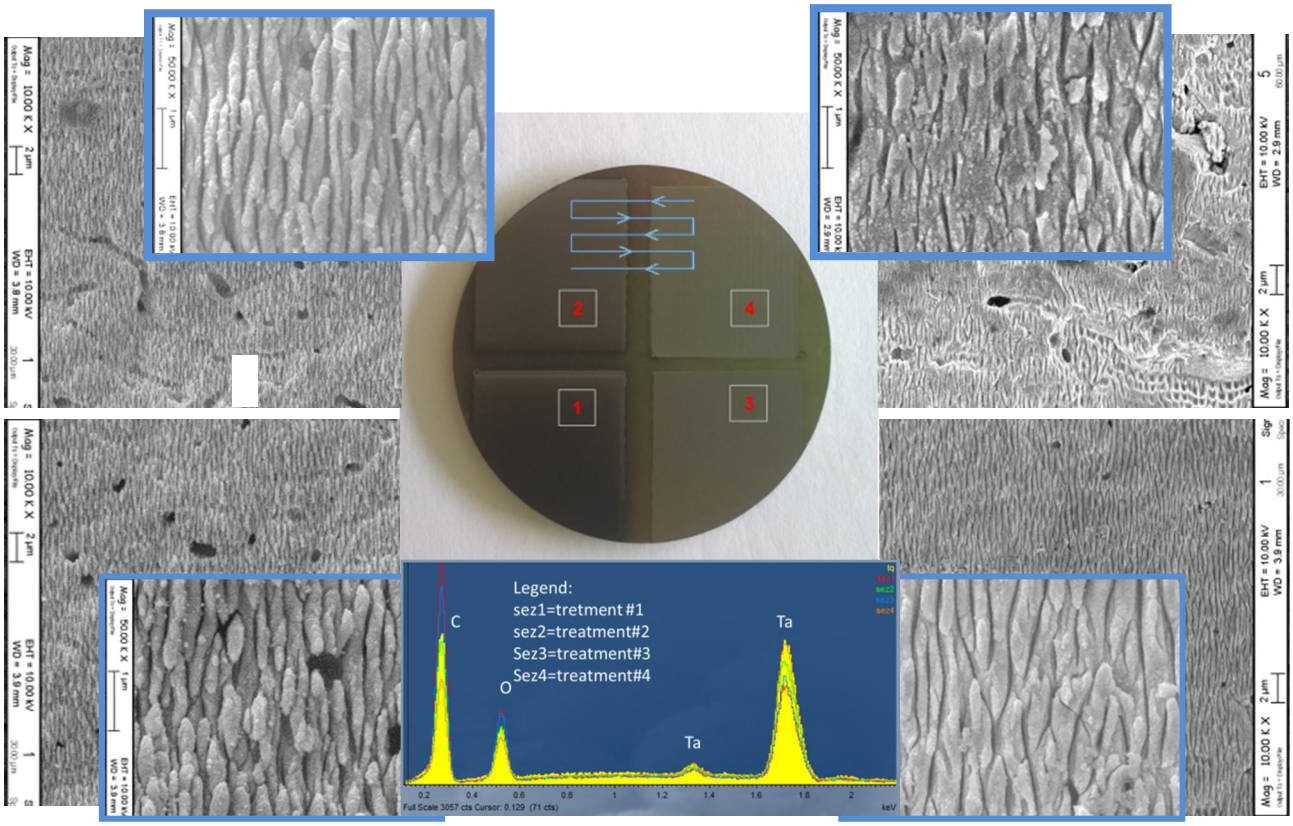

Figure 4: Microstructural features and corresponding EDS spectra of laser treated areas in sample T0.2

Figure 4 compares the surface morphologies obtained in the four tested combinations for sample T0.2. Inside the grooves, the appearance of a periodic structure is observed which is only interrupted in correspondence of pre-existent surface holes. For both samples, it can be observed that increasing the laser speed, i.e. decreasing the accumulated laser fluence, groves appear more regular and the tendency for formation of rounded precipitates decreases. The EDS analysis reveals an alteration in the relative intensities of Ta and C peaks, as well as a change of the O peak, the dependence of which on the accumulated fluence is not monotonic and will be studied in the near future. In detail, the slower the laser speed (treatment 1), the larger is the alteration of the Ta and C peaks. Following the same trend, Table II shows that the roughness R_a in the direction perpendicular to the laser scan progressively increases with the decrease in the laser scan (from treatment #4 to #1), due to longer permanence of the laser onto the material. For T0.2, R_a changes from 0.3 to 1 µm with decreasing the laser speed whilst for T1, the roughness changes from 1.2 to 2 µm. For the sake of clarity, however, the used profilometer gives approximate but representative values of the surface roughness induced by the submicrometric pattern, which mainly influences the material optical properties.
Figure 5 plots the roughness parameters R_a and R_t as a function of the accumulated laser fluence (Table I). We can appreciate that, for fixed sample, R_a and R_t show the same dependence on the

Paper published on:
Solar Energy Materials and Solar Cells, Vol. 161 (2017), pages 1-6,
http://dx.doi.org/10.1016/j.solmat.2016.10.054
http://www.sciencedirect.com/science/article/pii/S092702481630469X

fluence. We can also notice that the roughness increase is larger (about five times) for the smoother T0.2 material, while for sample T1 the roughness is doubled.

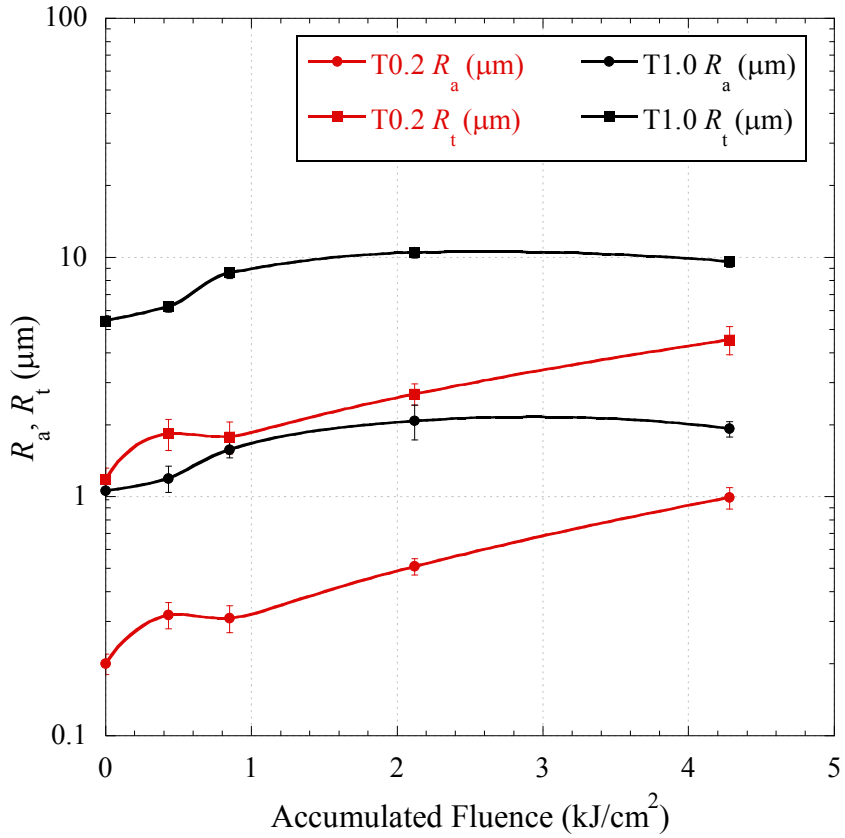

Figure 5: Roughness as a function of the laser accumulated fluence.

Optical properties

The acquired hemispherical reflectance spectra are shown in Figures 6 and 7. We can appreciate how the femtosecond laser texturing dramatically decreases the reflectance of samples. For instance, at 2 μm wavelength, the reflectance of T0.2 drops from the 71% value of the untreated surface to only 20% for T0.2#1. Similarly, for T1 series, the reflectance decreases from 65% (untreated surface) to 17% (T1#1). If we focus at around 0.55 μm wavelength, where the sunlight spectrum is maximum, we can see that going from as-polished surfaces to type-1 laser treatment, the reflectance decreases by five times for sample T0.2 and by ten times for sample T1. Again it can be noticed that the reflectance in the 1-6 μm range decreases progressively with increasing the accumulated fluence onto the surface (e.g. from treatments #4 to #1). This is probably due to either a morphological change; e.g. increase of roughness, or a compositional change e.g. different C/Ta ratio, which altered the intrinsic absorption characteristics of the starting material.

Paper published on:
Solar Energy Materials and Solar Cells, Vol. 161 (2017), pages 1-6,
http://dx.doi.org/10.1016/j.solmat.2016.10.054
http://www.sciencedirect.com/science/article/pii/S092702481630469X

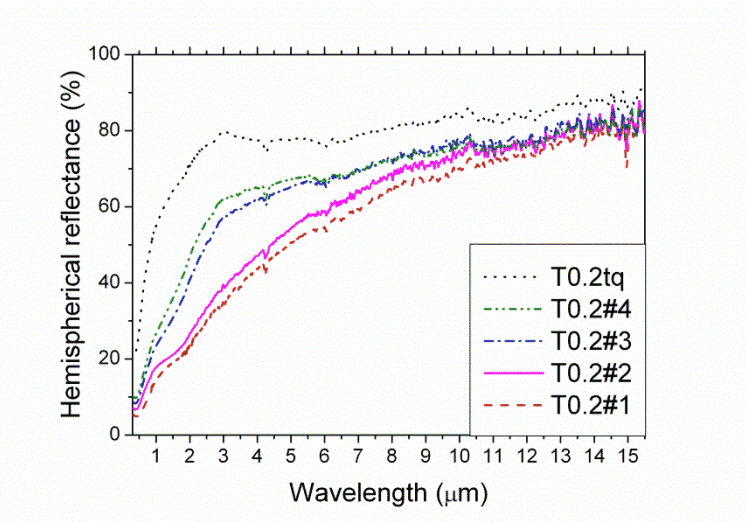

Figure 6: Reflectance spectra of sample T0.2.

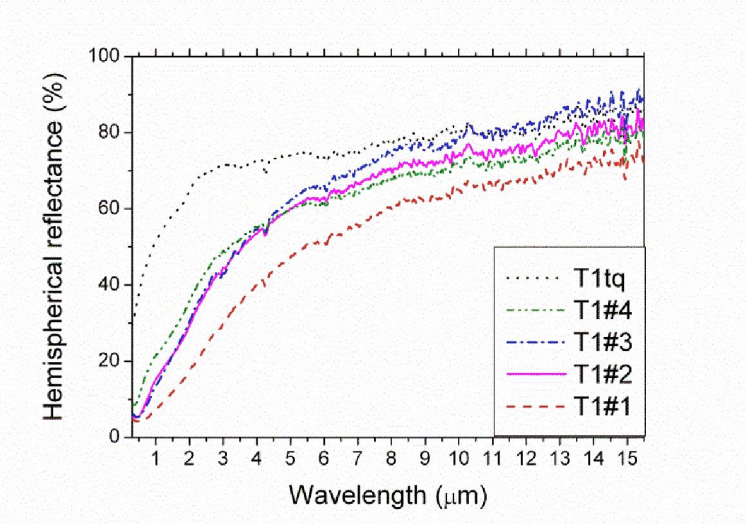

Figure 7: Reflectance spectra of sample T1.

If we compare T0.2 and T1 spectra, we can see that for T0.2 sample, which has the smoothest starting surface, the reflectance monotonically decreases on the whole investigated spectral range, while for the rougher T1 sample the behavior is not monotonic. This can be due to the fact that the response of a rough surface to a powerful laser beam can be intrinsically different from that of a smooth surface. In fact geometrical factors can arise, like locally non-normal incidence, with subsequent change in the laser beam absorption, secondary reflections onto the surface due to nearby roughness, radiation trapping, etc, which make the interaction more complicated with unpredictable effects.
For a quantitative evaluation of the impact of femtosecond laser texturing on optical properties, it is useful to calculate the total solar absorbance α and to estimate the hemispherical emittance ε at high temperature. These quantities can be obtained from the experimental room-temperature hemispherical reflectance $\rho^{\frown}(\lambda)$ according to the equations:

Paper published on:
Solar Energy Materials and Solar Cells, Vol. 161 (2017), pages 1-6,
http://dx.doi.org/10.1016/j.solmat.2016.10.054
http://www.sciencedirect.com/science/article/pii/S092702481630469X

$$\alpha = \frac{\int_{\lambda_{min}}^{\lambda_{max}} (1-\rho^{\frown}(\lambda)) \cdot S(\lambda) d\lambda}{\int_{\lambda_{min}}^{\lambda_{max}} S(\lambda) d\lambda}, \qquad (1)$$

where $S(\lambda)$ is the Sun emission spectrum [37] and the integration is carried out between $\lambda_{min} = 0.3$ µm and $\lambda_{max} = 3.0$ µm; and:

$$\varepsilon = \frac{\int_{\lambda 1}^{\lambda 2} (1-\rho^{\frown}(\lambda)) \cdot B(\lambda,T) d\lambda}{\int_{\lambda 1}^{\lambda 2} B(\lambda,T) d\lambda} \qquad (2)$$

where $B(\lambda,T)$ is the blackbody spectral radiance at the temperature T of interest and $\lambda 1 = 0.3$ µm and $\lambda 2 = 15.0$ µm. Let us consider for instance a temperature of 1200 K. The two main parameters to be taken into account for solar absorber applications are the solar absorbance α and the α/ε ratio (somewhere called spectral selectivity). Ideally, α should be the nearest as possible to unity, while α/ε should be taken as higher as possible. Figure 8 shows both values for the investigated surfaces.

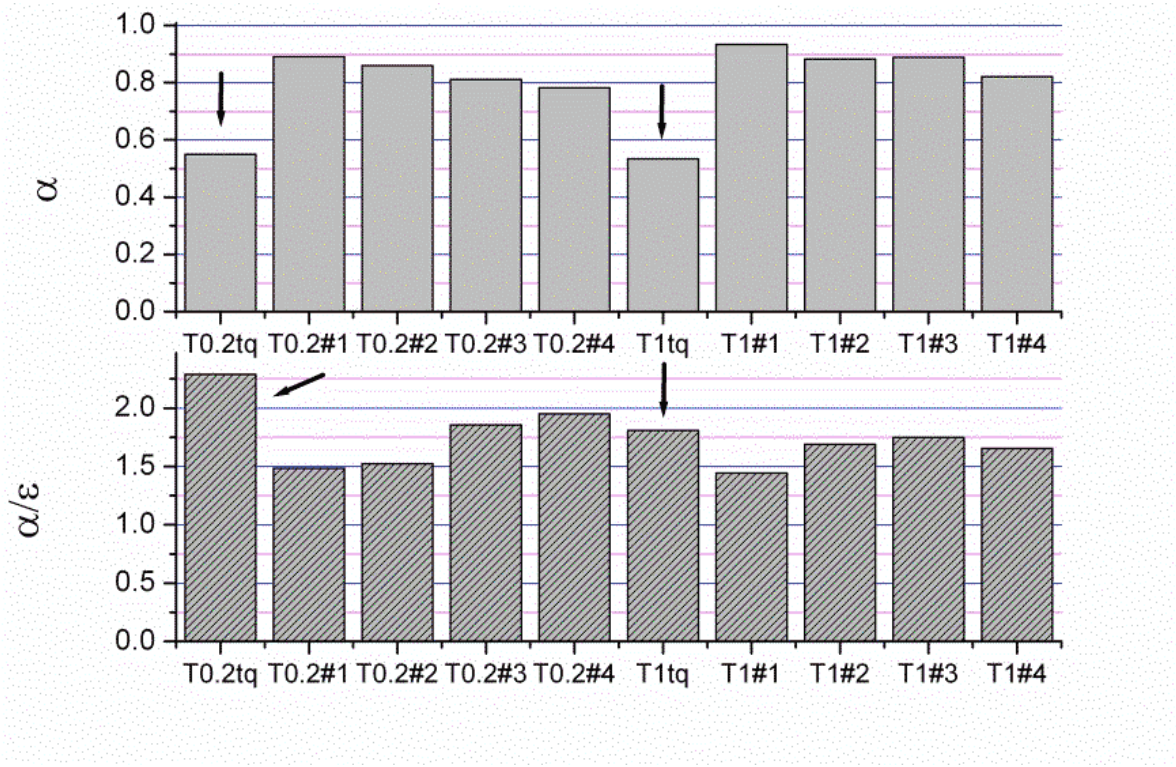

Figure 8: Solar absorbance α and spectral selectivity α/ε for the investigated surfaces. Arrows indicate untreated materials.

We can observe that for both investigated starting roughness levels, femtosecond laser texturing considerably increases the solar absorbance, which is nearly doubled. For both samples, α increased

Paper published on:
Solar Energy Materials and Solar Cells, Vol. 161 (2017), pages 1-6,
http://dx.doi.org/10.1016/j.solmat.2016.10.054
http://www.sciencedirect.com/science/article/pii/S092702481630469X

from ~0.5 for untreated surfaces to ~0.9 for areas treated with the higher fluence. The effect is larger in T1-based samples, where the original roughness was higher (α reaches 0.9 for three of four treated samples). However, laser texturing also decreases spectral selectivity because it generally decreases the value of the reflectance in intermediate wavelength regions 3-8 μm. If the comparison between the two investigated samples is concerned, we can see that T1, which is characterized, as untreated material, by a starting slightly lower spectral selectivity than T0.2, almost preserves its spectral selectivity with laser texturing, see sample T1#3 and, to a slightly lesser extent, also samples T1#2 and T1#4. For T0.2 samples the decrease of spectral selectivity is larger. Comparing the two plots in Figure 8, we can see that for both materials the longest interaction with laser (type 1-patterning) produces the largest increase in absorbance but also the largest decrease in spectral selectivity, which, in any case, remains higher (1.5 ÷ 1.4) than that of the most advanced material in solar absorbers to date, i.e. silicon carbide (SiC, $\alpha/\varepsilon \approx 1$) [10].

As a term of comparison, as we have mentioned in the introduction, untreated UHTCs are characterized by generally low solar absorbances (0.4 ÷ 0.7 for different carbides) and by spectral selectivities in the range 1.8 ÷ 2.8 [19]. Generally speaking, a high spectral selectivity is usually accompanied by a low solar absorbance and vice-versa. As for the comparison with similarly femtosecond-treated materials, our preliminary study on hafnium carbide [33] produced an increase in spectral selectivity ($\alpha/\varepsilon \approx 1.8$ and 2.1 for untreated and treated HfC, respectively) but almost no change in solar absorbance ($\alpha \approx 0.7$ in both cases). However it should be noticed the laser treatment was much milder for HfC than for the system described in the present work (the scan speed in [33] was as higher as 8 mm/s, to be compared to ≈ 5.6 mm/s for type-1 and 0.6 mm/s for type-4 tests of the present work.) This points out the importance to find optimized laser parameters, to obtain the best tradeoff between increased solar absorbance and spectral selectivity.

4. Conclusions

In this work we show the effect of femtosecond laser treatment on microstructure and optical properties of tantalum carbide pellets. As a function of the interaction time with laser radiation, different microstructural features can be obtained. During laser scan, periodic structures (grooves) are created in the perpendicular direction. Grooves are less regular and show more rounded precipitates as the interaction time between laser beam and ceramic material is increased. Correspondingly, the roughness is increased and the surface composition is altered, with changes of the Ta/C ratio. Laser treatments heavily affect optical properties of samples, in particular they considerably increase solar absorbance, showing thus promising perspectives for the use of such treated materials for solar energy applications. In fact, absorbance is considered the most important parameter for solar receiver materials. A secondary effect is the decrease of spectral selectivity, even if it is worth mentioning that it remains still higher than that of reference advanced solar absorbers (SiC). A further development of this work is the optimization of pattern parameters, to keep as much as possible the spectral selectivity of the starting material.

Acknowledgements
Part of this activity has been carried out in the framework of the STAGE-STE European project and "SOLE-2" project funded by the Italian bank foundation "Fondazione Ente Cassa di Risparmio di

Paper published on:
Solar Energy Materials and Solar Cells, Vol. 161 (2017), pages 1-6,
http://dx.doi.org/10.1016/j.solmat.2016.10.054
http://www.sciencedirect.com/science/article/pii/S092702481630469X

Firenze" (pratica n. 2014.0711). Thanks are due to C. Melandri and D. Dalle Fabbriche (CNR-ISTEC) and M. D'Uva and M. Pucci (CNR-INO) for technical assistance.

References

[1] E. Wuchina, E. Opila, M. Opeka, W. Fahrenholtz, I. Talmy, UHTCs: Ultra High temperature Ceramic Materials for Extreme Environment Applications, Interface 16[4] (2007) 30-6.
[2] A. Bellucci, P. Calvani, E. Cappelli, S. Orlando, D. Sciti, R. Yogev, A. Kribus, D. M. Trucchi; "Preliminary characterization of ST2G: Solar thermionic-thermoelectric generator for concentrating systems", 2015/6/23, NANOFORUM 2014 Conference Proceedings, 1667 (2015) 020007
[3] K. Burlafinger, A. Vetter, C. J. Brabec, Maximizing concentrated solar power (CSP) plant overall efficiencies by using spectral selective absorbers at optimal operation temperatures, Solar Energy 120 (2015) 428-438
[4] Y. Tian, C.Y. Zhao, A review of solar collectors and thermal energy storage in solar thermal applications, Applied energy 104 (2013) 538-553.
[5] C.E. Kennedy, Review of Mid- to High-temperature Solar Selective Absorber Materials, National Renewable Energy Laboratory, Technical report, 2002, pp.1-51.
[6] E. Sani, L. Mercatelli, F. Francini, J.-L. Sans, D. Sciti "Ultra-refractory ceramics for high-temperature solar absorbers", Scripta Materialia, vol. 65, pp. 775–778 (2011)
[7] Elisa Sani, Luca Mercatelli, Daniela Fontani, Jean-Louis Sans, Diletta Sciti " Hafnium and Tantalum Carbides for high temperature solar receivers", Journal of Renewable and Sustainable Energy vol. 3, 063107 (2011)
[8] Elisa Sani, Luca Mercatelli, Paola Sansoni, Laura Silvestroni, Diletta Sciti "Spectrally selective ultra-high temperature ceramic absorbers for high-temperature solar plants", Journal of Renewable and Sustainable Energy, vol. 4, 033104 (2012),
[9] E. Sani, L. Mercatelli, D. Jafrancesco, J.-L. Sans, D. Sciti "Ultra-High Temperature Ceramics for solar receivers: spectral and high-temperature emittance characterization", Journal of the European Optical Society: Rapid Publication, vol. 7, 12052 (2012)
[10] Diletta Sciti, Laura Silvestroni, Luca Mercatelli, Jean-Louis Sans, Elisa Sani "Suitability of ultra-refractory diboride ceramics as absorbers for solar energy applications", Solar Energy Materials and Solar Cells, vol. 109, pp. 8-16 (2013)
[11] Elisa Sani, Luca Mercatelli, Jean-Louis Sans, Laura Silvestroni, Diletta Sciti "Porous and dense Hafnium and Zirconium Ultra-High Temperature Ceramics for solar receivers", Optical Materials, vol. 36 (2013), 163–168.
[12] Elisa Sani, Marco Meucci, Luca Mercatelli, David Jafrancesco, Jean-Louis Sans, Laura Silvestroni, Diletta Sciti "Optical properties of boride ultrahigh-temperature ceramics for solar thermal absorbers", Journal of Photonics for Energy, vol. 4 (2014), 045599
[13] Sciti D., Silvestroni L., Sans J-L., Mercatelli L., Meucci M., Sani E., Tantalum diboride-based ceramics for bulk solar absorbers, Solar Energy Materials and Solar Cells, 130 (2014), 208-213
[14] E. Sani, E. Landi, D. Sciti, V. Medri, Optical properties of ZrB2 porous architectures, Solar Energy Materials and Solar Cells 144 (2016) 608-615.
[15] D. Sciti, L.Silvestroni, D.M.Trucchi, E.Cappelli, S.Orlando, E.Sani, Femtosecond laser treatments to tailor the optical properties of hafnium carbide for solar applications, Solar Energy Materials & Solar Cells 132 (2015) 460–466
[16] A. Bellucci, P. Calvani, E. Cappelli, S. Orlando, D. Sciti, R. Yogev, A. Kribus, D.M. Trucchi, Preliminary characterization of ST2G: Solar thermionic-thermoelectric generator for concentrating systems. In: 2015/6/23, NANOFORUM 2014 Conference Proceedings. 1667, 020007 (2015)

Paper published on:
Solar Energy Materials and Solar Cells, Vol. 161 (2017), pages 1-6,
http://dx.doi.org/10.1016/j.solmat.2016.10.054
http://www.sciencedirect.com/science/article/pii/S092702481630469X

[17] D. Sciti, L. Silvestroni, S. Guicciardi, D. dalle Fabbriche, A. Bellosi, Processing, mechanical properties and oxidation behavior of TaC and HfC composites containing 15 vol% $TaSi_2$ or $MoSi_2$, J. Of Mat. Res, 25, 6, 2056-65 (2009).
[18] L. Silvestroni, D. Sciti, Sintering Behavior, Microstructure, and Mechanical Properties: A Comparison among Pressureless Sintered Ultra-Refractory Carbides, Advanced in Materials Science and Engineering, vol. 2010, article ID 835018, 11 pages.
[19] E. Sani, L. Mercatelli, M. Meucci, A. Balbo, L. Silvestroni, D. Sciti, "Compositional dependence of optical properties of zirconium, hafnium and tantalum carbides for solar absorber applications", Solar Energy 131 (2016), 199–207
[20] G. Pellegrini, Experimental methods for the preparation of selectively absorbing textured surfaces for photothermal solar conversion, Solar Energy Materials 3 (1980) 391-404.
[21] A. Kumar Dubey, V. Yadava, Laser beam machining - A review, International Journal of Machine Tools & Manufacture 48 (2008) 609-628.
[22] A.N. Samant, N.B. Dahotre, Laser machining of structural ceramics—A review, Journal of the European Ceramic Society, 29 (2009) 969-993.
[23] T. R. Jervis, M. Natasi, K. M. Hubbard and J. – P. Hirvonen, Excimer laser surface processing of ceramics: process and properties. Journal of the American Ceramic Society; 76 (1993) 350-355.
[24] F. Valentini, I. Zambotto, D. Sciti, L. Silvestroni, C. Melandri, S. Guicciardi, "Microstructure and Nanoindentation properties of surface textures obtained by laser machining and molding in silicon carbide", Advanced Engineering Materials; 15 (2013) 330-335
[25] D. Sciti, A. Bellosi, "Laser-induced surface drilling of silicon carbide ", Applied Surface Science, 180 1-2 (2001) 92-101.
[26] J. Lumpp and S. D. Allen, Excimer-laser ablation of aluminum nitride, Journal of Materials Research 12 (1997) 218-225.
[27] S. Cao, A. J. Pedraza, L. F. Allard, Laser-induced microstructural changes and decomposition of aluminum nitride, Journal of Materials Research 10 (1995) 54 -62.
[28] L. Y. Sadler, M. Shamsuzzoha, Response of silicon carbide to high-intensity laser irradiation in a high-pressure inert gas atmosphere, Journal of Materials Research 12 (1997) 147-160
[29] E. Cappelli, S. Orlando, D. Sciti, M. Montozzi, L. Pandolfi, "Ceramic surface modifications induced by pulsed laser treatments", Applied Surface Science, Vol. 154 -155 (2000) 682-688
[30] Laser Processing of Materials: Fundamentals, Applications and Developments, Peter Schaaf (Editor), Springer Series in Materials Science, pp.1-248, Springer 2010.
[31] P. Calvani, A. Bellucci, M. Girolami, S. Orlando, V. Valentini, A. Lettino, and D.M. Trucchi, Optical Properties of Femtosecond Laser Treated Diamond, Applied Physics A, 117 (2014) 25-29
[32] P. Calvani, A. Bellucci, M. Girolami, S. Orlando, V. Valentini, R. Polini, D. M. Trucchi, Black diamond for solar energy conversion, Carbon 105 (2016) 401-407
[33] D. Sciti, L. Silvestroni, D.M. Trucchi, E. Cappelli, S. Orlando, E. Sani, Femtosecond laser treatments to tailor the optical properties of hafnium carbide for solar applications, Solar Energy Materials & Solar Cells 132 (2015) 460–466.
[34] J. Eichstädt, G.R.B.E. Römer, A.J. Huis in 't Veld, Determination of irradiation parameters for laser-induced periodic surface structures, Applied Surface Science, 264 (2013) 79-87
[35] J.M. Liu, Simple Technique for measurements of pulsed Gaussian-beam spot sizes, Optics Letters, 7 (1982) 196-198;
[36] J. Bonse, S. Baudach, J. Krüger, W. Kautek, M. Lenzner, Femtosecond laser ablation of silicon–modification thresholds and morphology, Applied Physics A, 74 (2002) 19-25
[37] Standard Tables for Reference Solar Spectral Irradiances: Direct Normal and Hemispherical on 37° Tilted Surface, Active Standard ASTM G173. ASTM G173–03(2012)